UCRL-ID-148053

Prediction of Failure Due to Thermal Aging, Corrosion and Environmental Fracture in Amorphous and Titanium Alloys

J. C. Farmer

April 15, 2002

U.S. Department of Energy

Lawrence
Livermore
National
Laboratory

DISCLAIMER

This work was performed under the auspices of the U. S. Department of Energy by the University of California, Lawrence Livermore National Laboratory under Contract No. W-7405-Eng-48.

Prediction of Failure Due to Thermal Aging, Corrosion and Environmental Fracture in Amorphous and Titanium Alloys

Prepared for:

Dr. Leo Christodoulou, Program Manager, Materials, DARPA/DSO, 3701 North Fairfax Drive, Arlington, Virginia 22203-1714, Telephone 703-696-2374, Fax 703-696-3999, Email lchristodoulou@darpa.mil

Dr. A. C. "Chip" Smith, Jr., Research Director, Directed Technologies, 3601 Wilson Boulevard, Suite 650, Arlington, Virginia 22201, Telephone 703-243-3383, Fax 703-243-2724, Email Chip_Smith@DirectedTechnologies.com

Prepared by:

Dr. Joseph C. Farmer, Directorate Senior Scientist, Chemistry and Materials Science, Lawrence Livermore National Laboratory Livermore, California 94550, Telephone 925-423-6574, Email *farmer4@llnl.gov*

Introduction

DARPA is exploring a number of advanced materials for military applications, including amorphous metals and titanium-based alloys. Equipment made from these materials can undergo degradation due to thermal aging, uniform corrosion, pitting, crevice corrosion, denting, stress corrosion cracking, corrosion fatigue, hydrogen induced cracking and microbial influenced corrosion. Amorphous alloys have exceptional resistance to corrosion, due in part to the absence of grain boundaries, but can undergo crystallization and other phase instabilities during heating and welding. Titanium alloys are extremely corrosion resistant due to the formation of a tenacious passive film of titanium oxide, but is prone to hydrogen absorption in crevices, and hydrogen induced cracking after hydrogen absorption. Accurate predictions of equipment reliability, necessary for strategic planning, requires integrated models that account for all relevant modes of attack, and that can make probabilistic predictions. Once developed, model parameters must be determined experimentally, and the validity of models must be established through careful laboratory and field tests. Such validation testing requires state-of-the-art surface analytical techniques, as well as electrochemical and fracture mechanics tests.

The interaction between those processes that perturb the local environment on a surface and those that alter metallurgical condition must be integrated in predictive models. The material and environment come together to drive various modes of corrosive attack (Figure 1). Models must be supported through comprehensive materials testing capabilities. Such capabilities are available at LLNL and include: the Long Term Corrosion Test Facility (LTCTF) where large numbers of standard samples can be exposed to realistic test media at several temperature levels; a reverse DC machine that can be used to monitor the propagation of stress corrosion cracking (SCC) *in situ*; and banks of potentiostats with temperature controlled cells for potentiostatic and potentiodynamic testing (Figure 2).

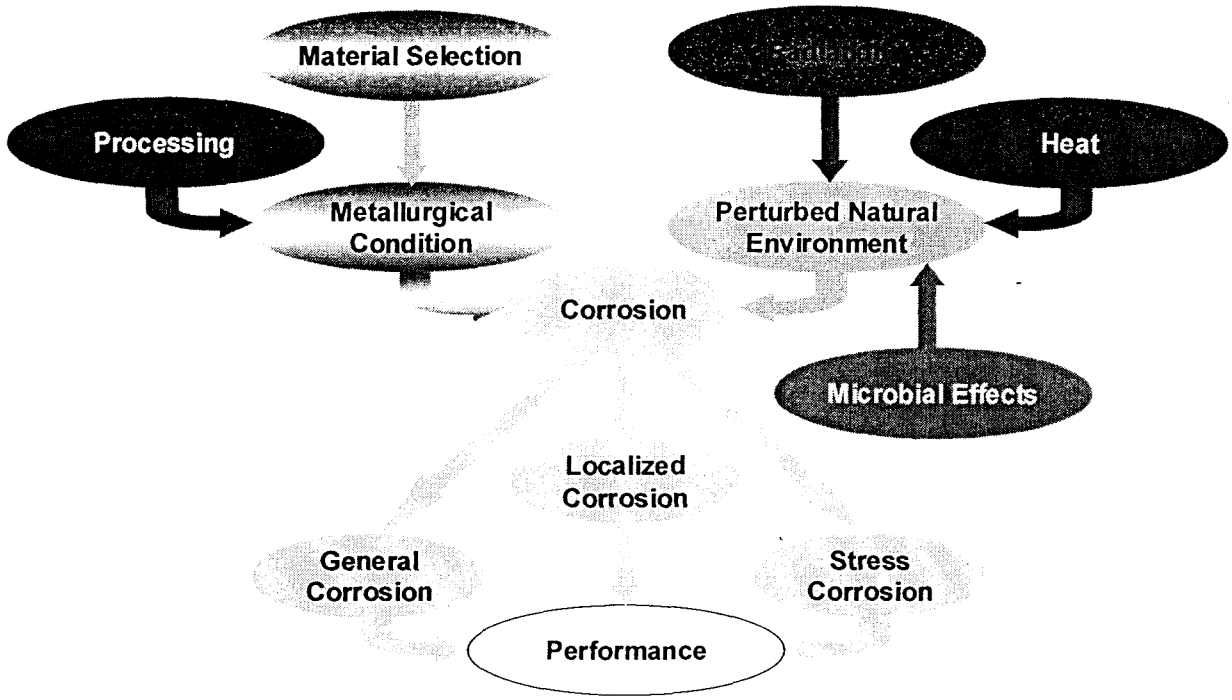

Figure 1. The interaction between those processes that perturb the local environment on a surface, and those which alter metallurgical condition. The material and environment come together to drive various modes of corrosive attack.

Lawrence Livermore National Laboratory (LLNL) has developed substantial expertise in the detection, quantification, prediction and mitigation of corrosion-related materials failure, and is well prepared to address this important problem. The LLNL corrosion laboratory has the capability of studying general and localized corrosion with classical methods, such as linear polarization, electrochemical impedance spectroscopy, weight loss, scanning electron microscopy, and slow-strain rate testing. However, capabilities unique to LLNL also exist. These include thermal gravimetric analysis, transmission electron microscopy, *in situ* and *ex situ* atomic force microscopy (conventional and tunneling), X-ray photoelectron spectroscopy, low-angle X-ray diffraction, Raman microprobe, various *in situ* micro-sensors, and other methodologies.

Thousands of corrosion samples are exposed to high-temperature saturated brines in the Long Term Corrosion Test Facility

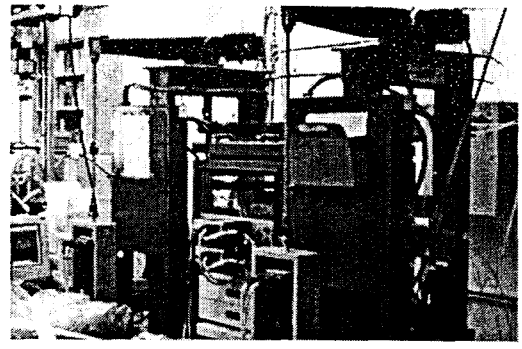

Propagation of stress corrosion cracks (SCC) is monitored *in situ* with the Reverse DC Technique

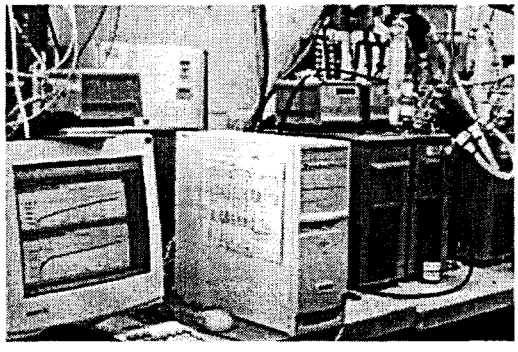

Arrays of potentiostats are used to measure threshold potentials for localized corrosion & the time-evolution of the corrosion potential

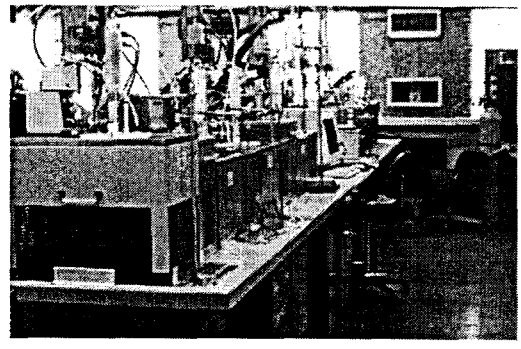

Figure 2. Illustration of some of the materials testing capabilities at LLNL including: the Long Term Corrosion Test Facility (LTCTF) where large numbers of standard samples can be exposed to realistic test media at several temperature levels; a reverse DC machine that can be used to monitor the propagation of stress corrosion cracking (SCC) *in situ*; and banks of potentiostats with temperature controlled cells for potentiostatic and potentiodynamic testing.

Probabilistic models have been developed to account for the stochastic nature of the pit initiation, while deterministic models have been developed to calculate transient ion concentrations within crevices and pits. These deterministic and probabilistic models that can be used to predict the thresholds of localized corrosion, pit density, and local penetration rate. Experimental measurements serve as inputs for the models.

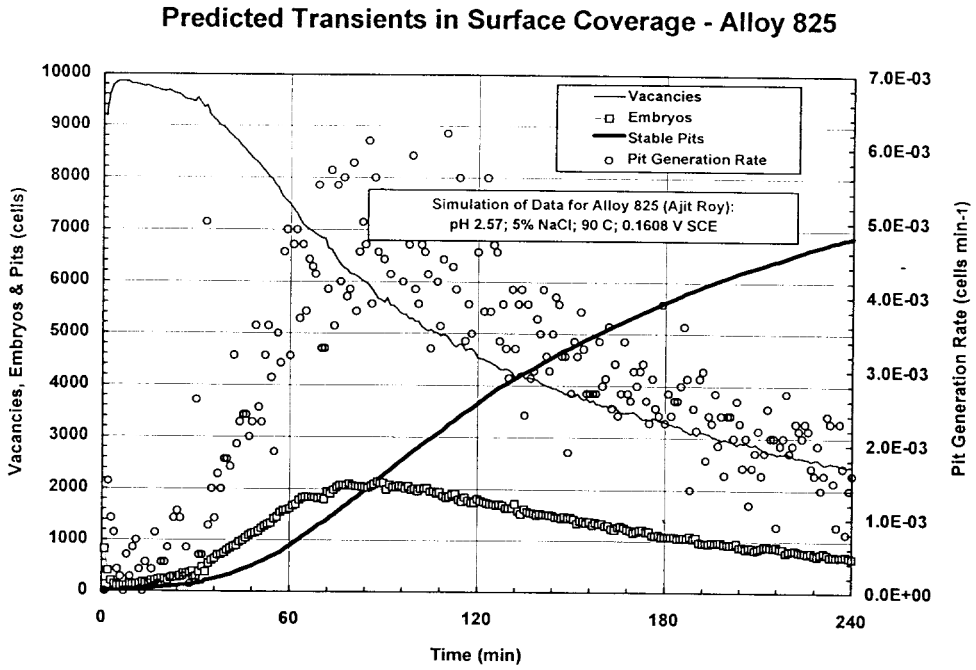

Figure 3. Probabilistic pitting models have been developed, based upon the stochastic approaches of Shibata, to predict transients in the density of vacancies, embryos and stable pits for a variety of materials, including Alloy 825.

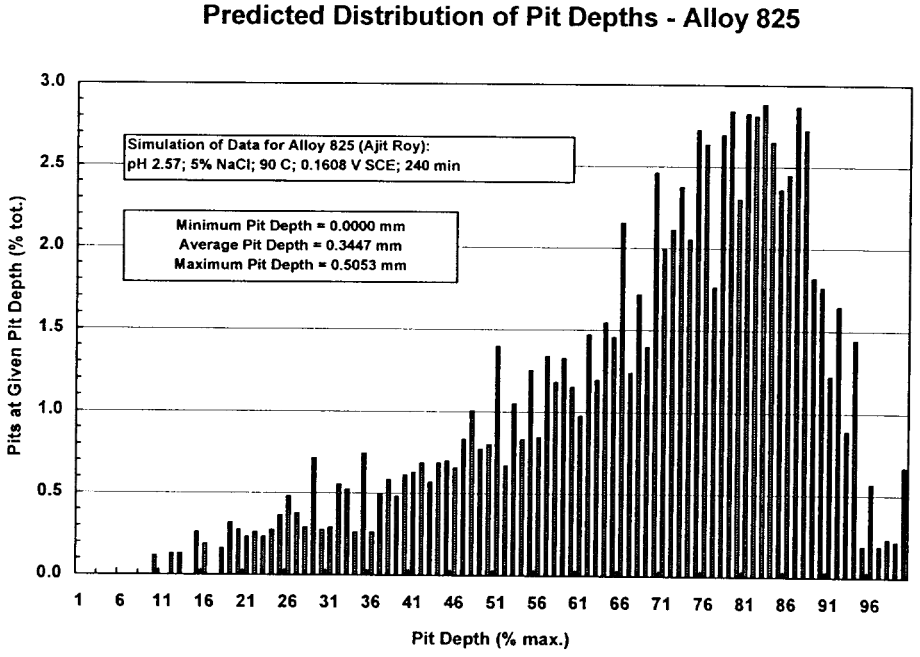

Figure 4. These same models predict distributions of pit depth as a function of time, with a prediction shown here for Alloy 825.

An integrated model for total system performance assessment, which accounts for the various modes of failure has also been developed. This is a probabilistic model, with individual components based upon mechanistic process-level models. This model can predict cumulative distribution functions for failure time, given various transient input parameters. Some details are discussed in subsequent sections.

Definition of Local Environments

In power generation equipment, electronics, naval ships and structures, airplanes and helicopters, land vehicles, pipelines, desalination and water purification equipment, the rate of degradation is determined largely by the evolution of local environments found on exposed surfaces, underneath paint coatings, on heat-exchanger surfaces, and inside crevices and other occluded areas, including lap joints and rivets. The deposition of scale on heat exchanger surfaces minimizes thermal efficiency, makes it necessary for materials to be operated at higher temperature than would be otherwise desirable, and promotes under-deposit corrosion. The process control technologies necessary to mitigate such undesirable effects are also available at LLNL, and include dynamic simulators, thermo-chemical codes for predicting water chemistry at elevated temperature and pressure, and corrosion sensor techniques that can be used to detect extremely small changes in penetration or oxide thickness. Dynamic process simulation, coupled with on-line real-time process sensors, and associated codes for the prediction of water chemistry and materials failure, have the potential of minimizing untimely equipment failure.

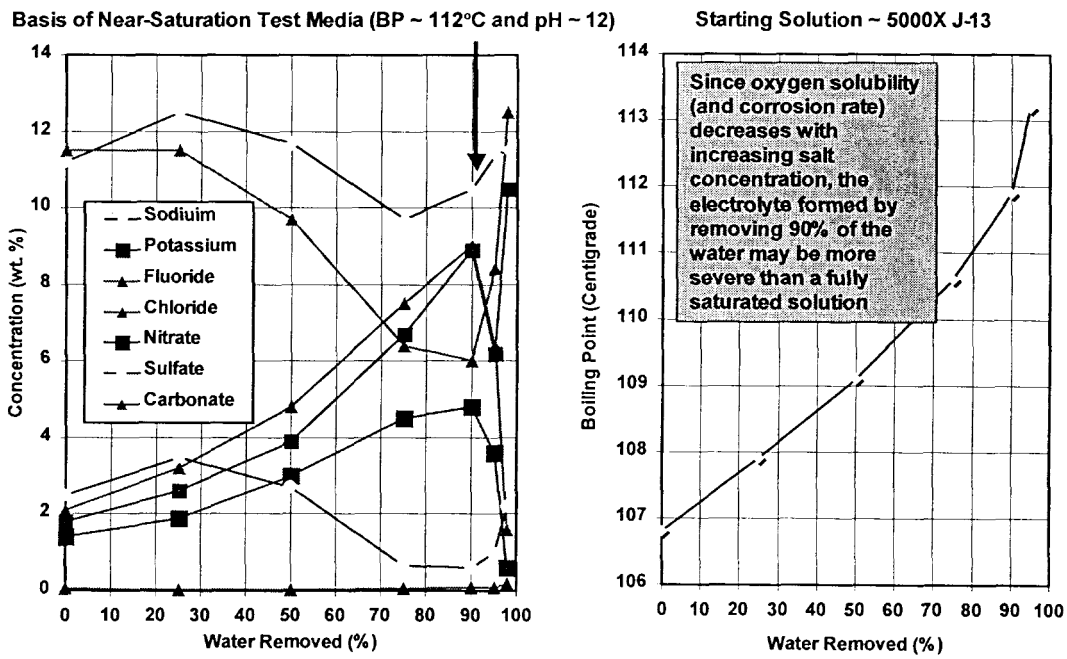

Figure 5. Evaporative concentration is used to establish the compositions of realistic test environments used to mimic those found on heat-transfer surfaces.

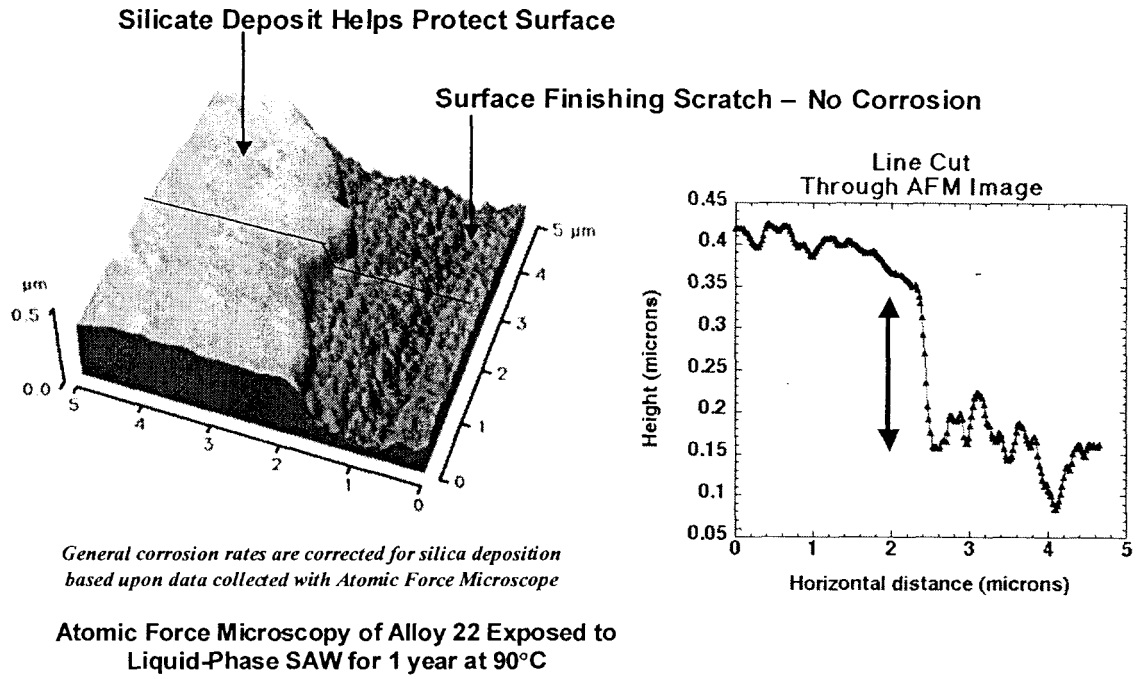

Figure 6. The thinnest of deposits on metal surfaces can be quantified through the use of atomic force microscopy.

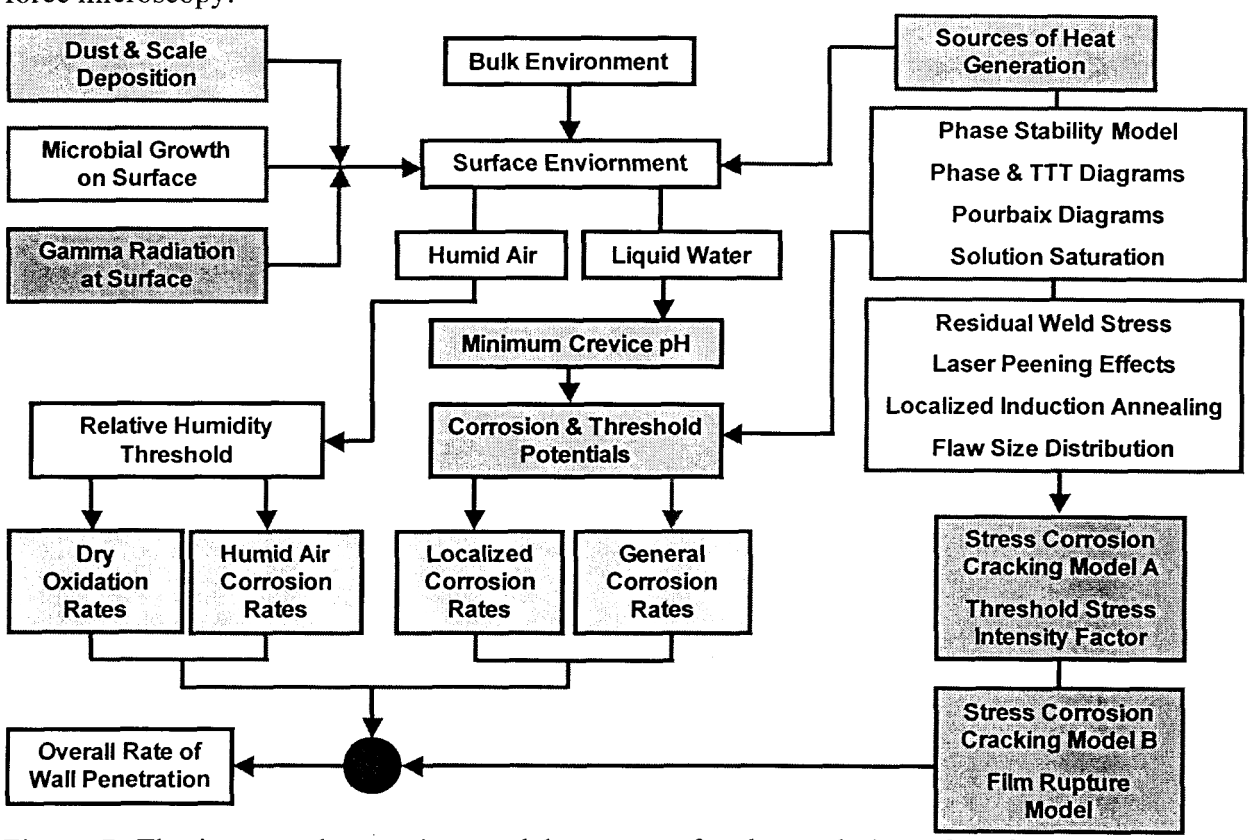

Figure 7. The integrated corrosion model accounts for the evolution of surface environments, thermal aging of the material, all known modes of corrosion and environmental cracking.

Aging and Phase Stability of Materials

Amorphous alloys are glassy, meta-stable materials that undergo crystallization if heated excessively. The thermodynamics and kinetics of these glass-to-crystalline transitions must be thoroughly understood in order to predict the elevated-temperature and long-term behavior of these materials. The kinetics of crystallization and precipitation can be quantified with *in situ* transient X-ray diffraction on a hot stage. Once formed, crystallites and precipitates can be further characterized with scanning electron microscopy, as well as transmission electron microscopy. Advanced thermo-chemical computer codes are used to predict phase diagrams, diagrams that serve as the scientific basis for determining whether or not undesirable phases will form under a particular set of conditions. Kinetic models are then used to determine the rate at which these undesirable phases form.

In the case of titanium alloys, hydrogen absorption and internal oxidation can also be quantified through the application of electron microscopy, secondary ion mass spectrometry, and the use of atomic force microscopy to image sub-surface hydrogen micro-bubbles in creviced regions.

In classical stainless steels and nickel-chromium-molybdenum alloys, thermal histories can result in the formation of a variety of undesirable precipitates that deplete those alloying elements responsible for exceptional passivity. Since these precipitates may be rich in molybdenum and chromium, two of the alloying elements responsible for passivity, aging can also result in increased susceptibility to general and localized corrosion, as well as to stress corrosion cracking and corrosion fatigue. Such precipitates can form within the individual grains or at grain boundaries, and can cause embrittlement.

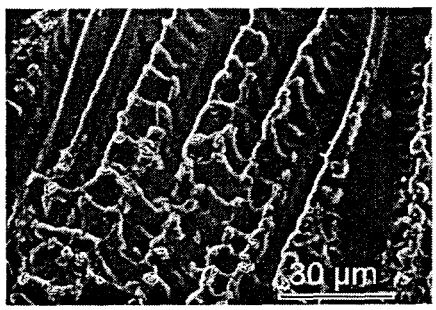

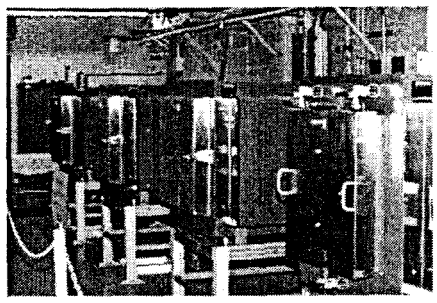

Phase stability studies have included identification of precipitates in base metal and welds, quantification of the rate of precipitation as a function of temperature, and theoretical kinetic and thermodynamic modeling

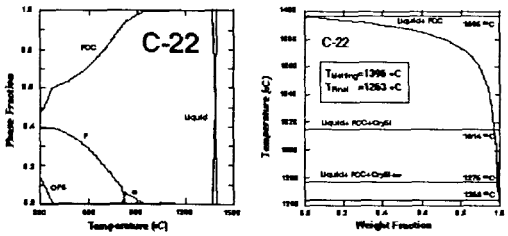

Alloy 22 aged over 4.5 years has been characterized to determine likelihood of phase instabilities occurring under expected repository conditions

The data do not indicate that such instabilities will occur. An aging facility is currently in operation, with future efforts focusing on cold worked and welded alloy 22

Figure 8. Metallic alloys undergo thermal aging in the LLNL Long Term Aging Facility (LTAF). The THERMOCALC code has been used to predict phase diagrams for nickel-chromium-molybdenum alloys, such as Hastelloy C-22.

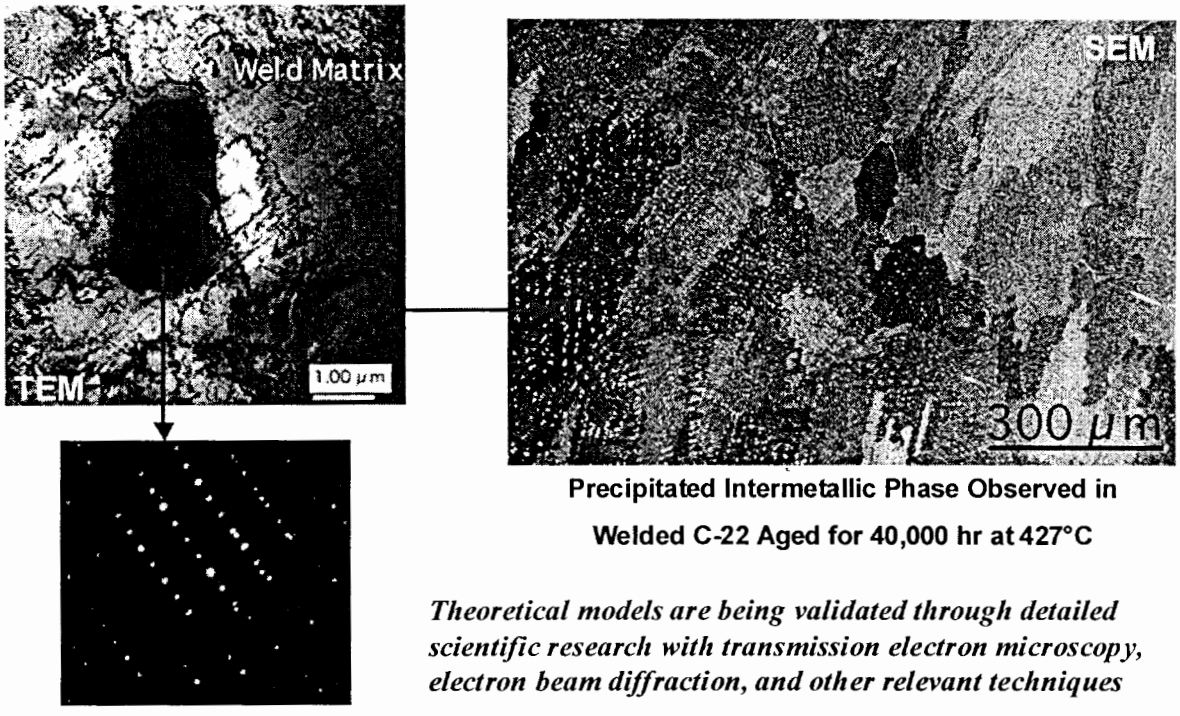

Figure 9. Intermetallic precipitates that form during extreme aging can be seen with the transmission electron microscope, with specific phases identified through the indexing of electron beam diffraction patterns.

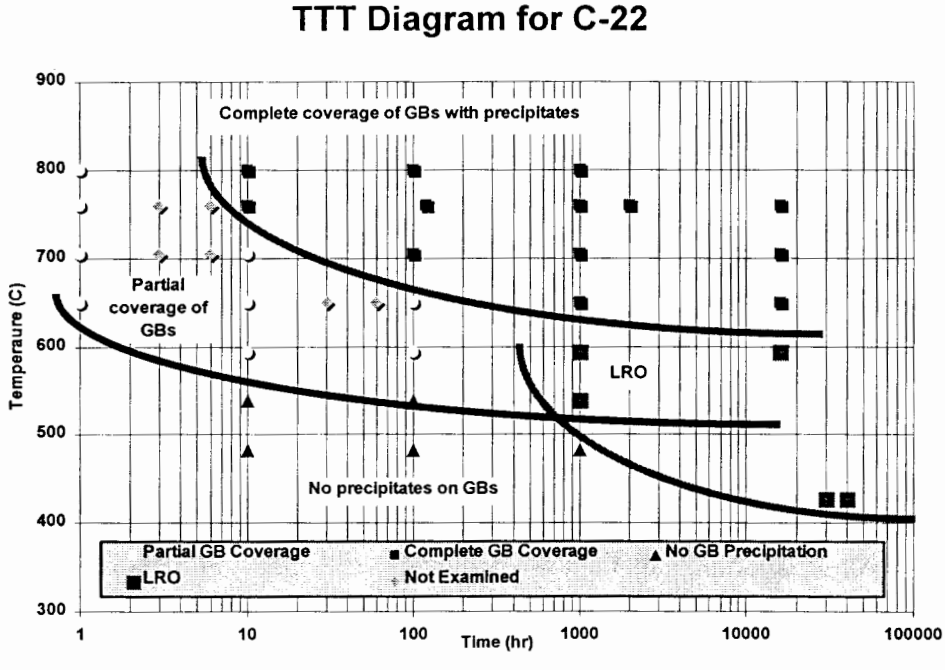

Figure 10. TEM data such as that shown in Figure 8 is then used to validate TTT curves.

General and Localized Corrosion

The corrosive attack of amorphous metals, titanium-based materials, and other alloys can be categorized as either general or localized corrosion. General corrosion results in the oxidation or active dissolution of a metal over an entire surface, whereas localized corrosion occurs over a relatively small area and is usually more severe (high penetration rates). Modes of localized corrosion include pitting, crevice corrosion, and inter-granular attack. These localized modes of attack are triggered above threshold values of temperature, electrochemical potential, pH and chloride ion concentration. Arrays of potentiostats and temperature-controlled electrochemical cells are available in the corrosion laboratories at LLNL for the precise determination of thresholds for localized attack. Some ions can buffer acidification due to metal hydrolysis reactions, while other ions serve as corrosion inhibitors at the metals surface. Micro-sensors have been developed to quantify the extent of pH lowering under deposits and in crevices. Autoclaves can be used for work at elevated temperature and pressure. Atomic force microscopy with an electrochemical stage is used available to study incipient corrosion, both *ex situ* and *in situ* with an electrochemical stage. X-ray photoelectron spectroscopy is used to determine passive film composition, as well as the oxidation state of the metal cations within the film.

The duplex structure of the oxide film during the high-temperature oxidation of Hastelloy C-22 is revealed through cross-sectional TEM with EDS profiling (Figure 11). The rates of corrosion and oxidation of alloys such as C-22 and Ti Gr 12 are extremely low, and require the development of special techniques for laboratory quantification in reasonable times. Photolithography has been used to establish gauge (reference) surfaces against which the thickness of oxide films, or the penetration due to dissolution, can be compared (Figure 12). Cyclic polarization is used to determine critical potentials where passive film stability is lost, and pitting initiates (Figure 13). After the conditions for pit initiation are known, the atomic force microscope (AFM) can be used to take "time lapse" images of the surface undergoing localized attack (Figure 14). During cyclic polarization of Hastelloy C-22 in alkaline brines, an anodic oxidation peak has been observed. X-ray photoelectron spectroscopy has been used to show that this electrochemical reaction is associated with the conversion of Mo(IV) to Mo(VI) (Figure 15). Changes in the passive film morphology associated with the anodic oxidation peak can be observed with the AFM, with a tenacious protective film observed below the anodic peak, and a porous film formed above (Figure 16). The occluded geometry of a crevice can cause acidification of the solution contained therein, due to field-driven electromigration of hydrogen and chloride ions, and to the hydrolysis reactions of dissolved metal cations inside the crevice. These effects have been simulated with finite element models (E_{pit} is the potential where the passive film is assumed to breakdown) (Figure 17). Transient pH profiles have been measured for a variety of alloys and environments, and have been used as a basis of validating predictive models (Figure 18). Crevice pH data show that in situations with buffer and inhibitor ions present, no lowering of the pH occurs (Figure 19). The impact of inhibitor and buffer ions on the crevice corrosion of materials with extreme resistance to localized has also been elucidated, finding that such species prevent crevice corrosion. Solutions of chloride salt near saturation, at similar potential and temperature, undergo crevice attack (Figure 20). The AFM has been used to observe the crevice attack of titanium alloys exposed to environments with concentrated fluoride salts (Figure 21). Secondary ion mass spectrometry has been used to measure the hydrogen absorbed by titanium in realistic crevice geometries (Figure 22). Once the hydrogen is absorbed, it can drive hydrogen induced cracking, diffusing down stress gradients.

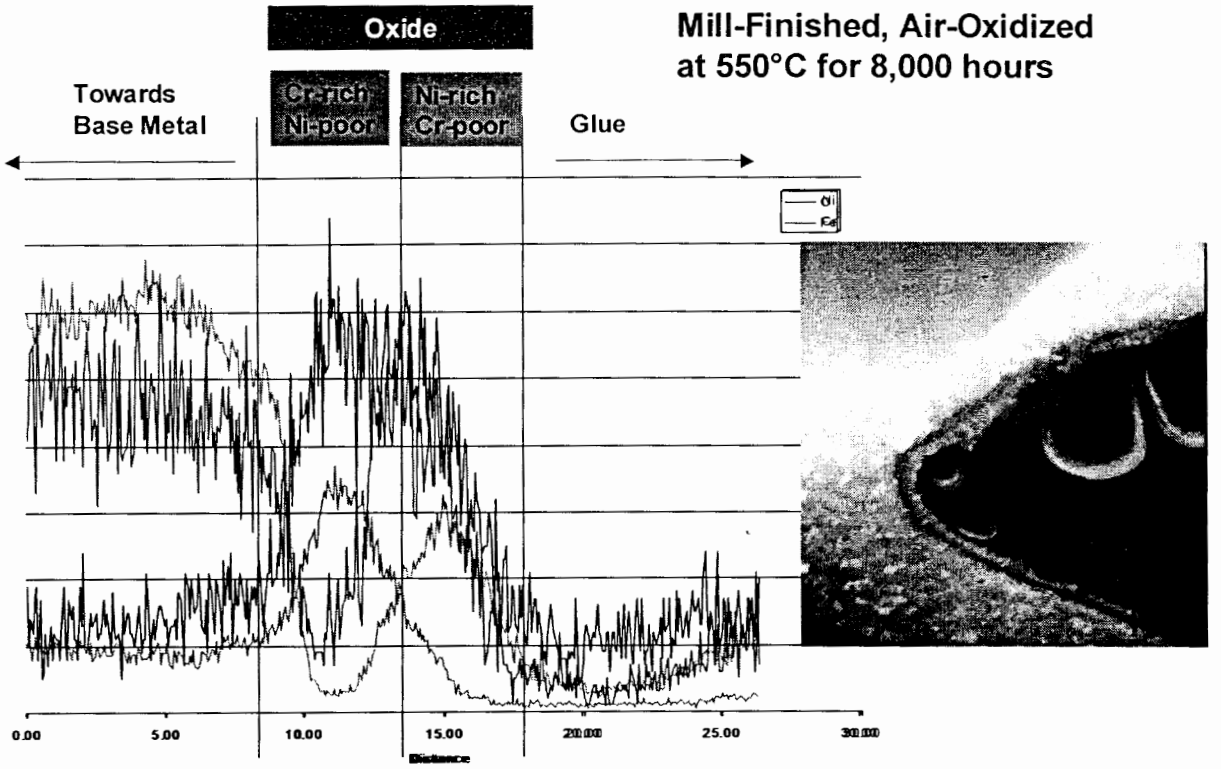

Figure 11. The duplex structure of the oxide film during the high-temperature oxidation of Hastelloy C-22 is revealed through cross-sectional TEM with EDS profiling.

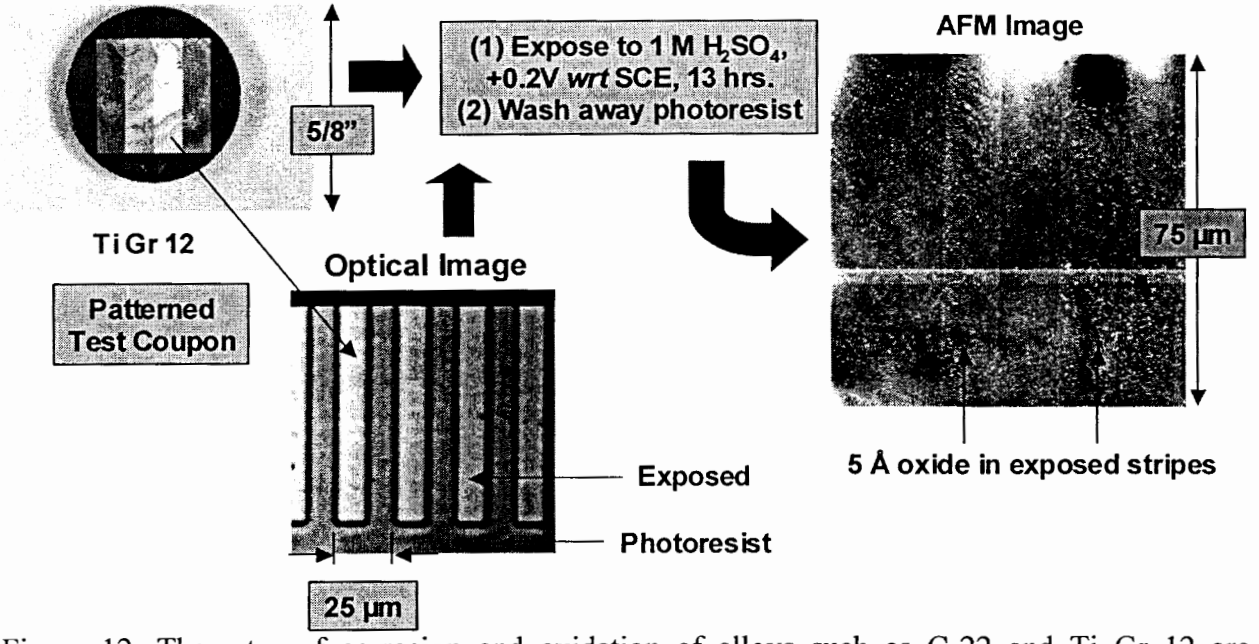

Figure 12. The rates of corrosion and oxidation of alloys such as C-22 and Ti Gr 12 are extremely low, and require the development of special techniques for laboratory quantification in reasonable times. Photolithography has been used to establish gauge (reference) surfaces against which the thickness of oxide films, or the penetration due to dissolution, can be compared.

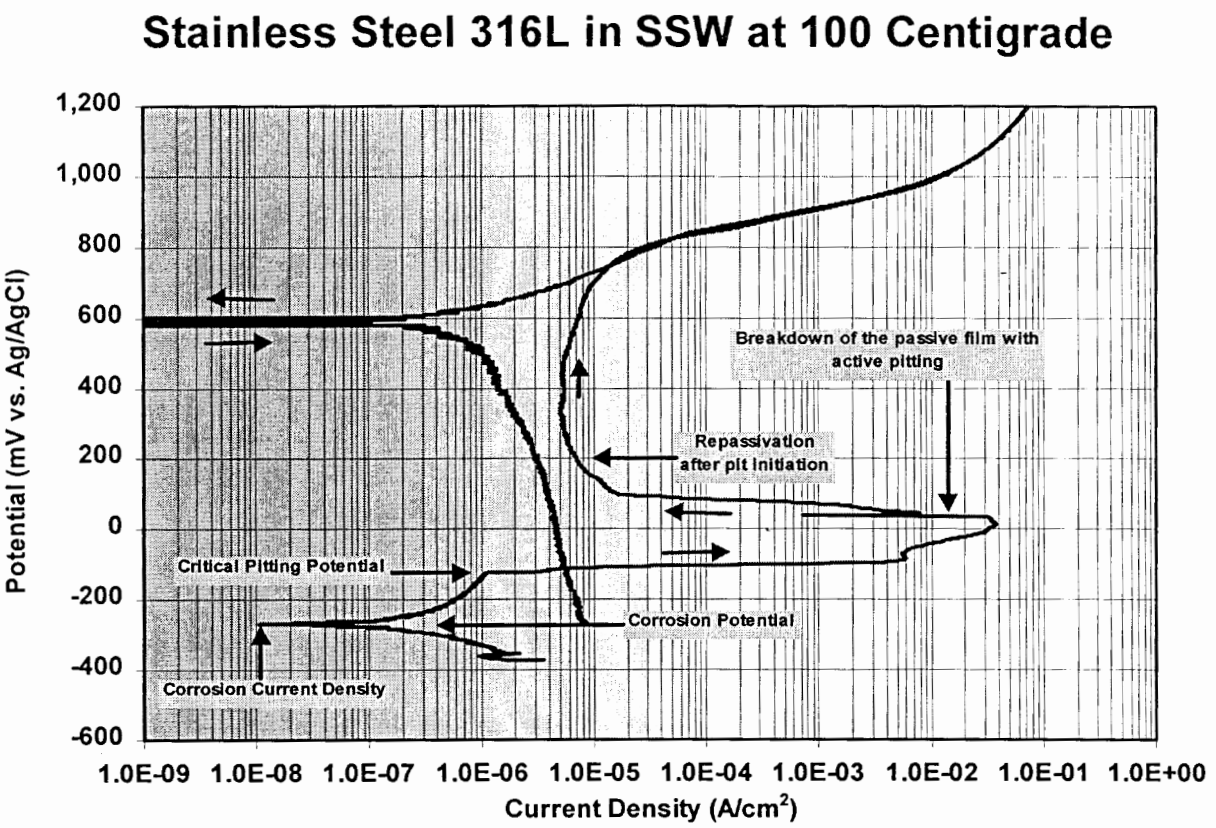

Figure 13. Cyclic polarization is used to determine critical potentials where passive film stability is lost, and pitting initiates.

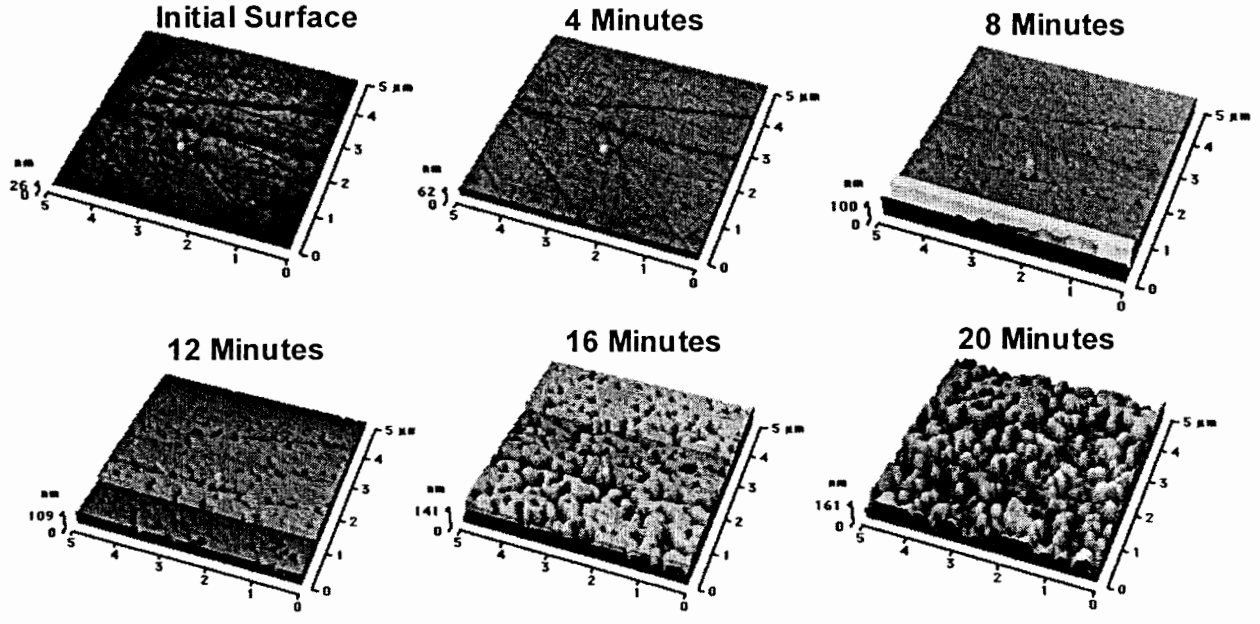

Figure 14. After the conditions for pit initiation are known, the atomic force microscope (AFM) ~~and~~ be used to take "time lapse" images of the surface undergoing localized attack.
CAN

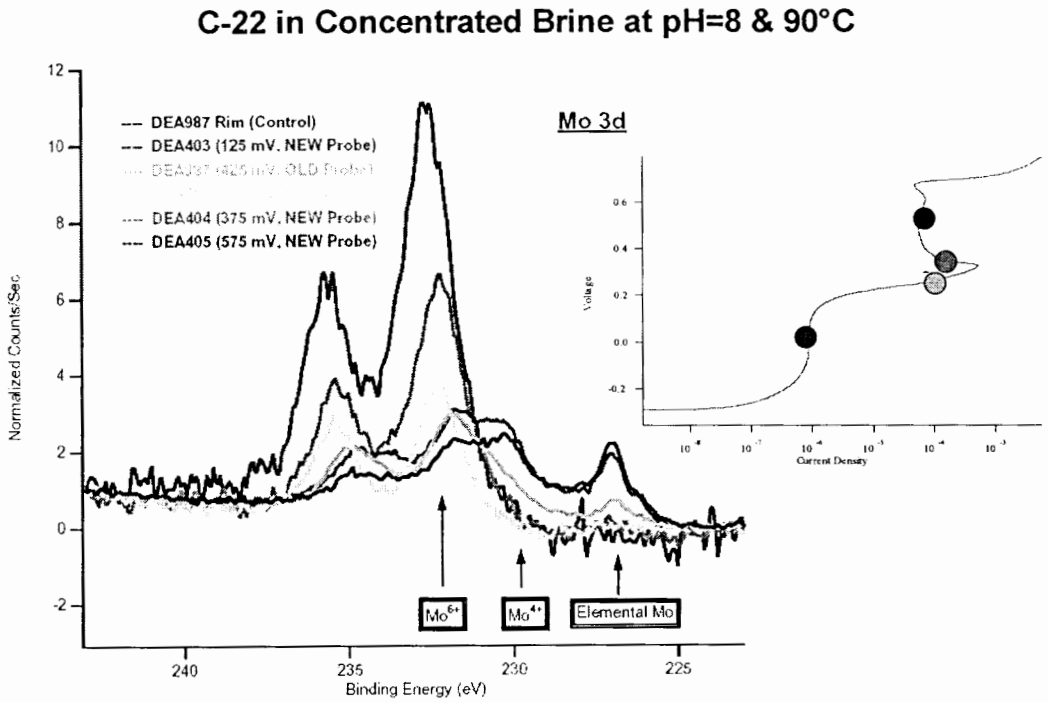

Figure 15. During cyclic polarization of Hastelloy C-22 in alkaline brines, an anodic oxidation peak has been observed. X-ray photoelectron spectroscopy has been used to show that this electrochemical reaction is associated with the conversion of Mo(IV) to Mo(VI).

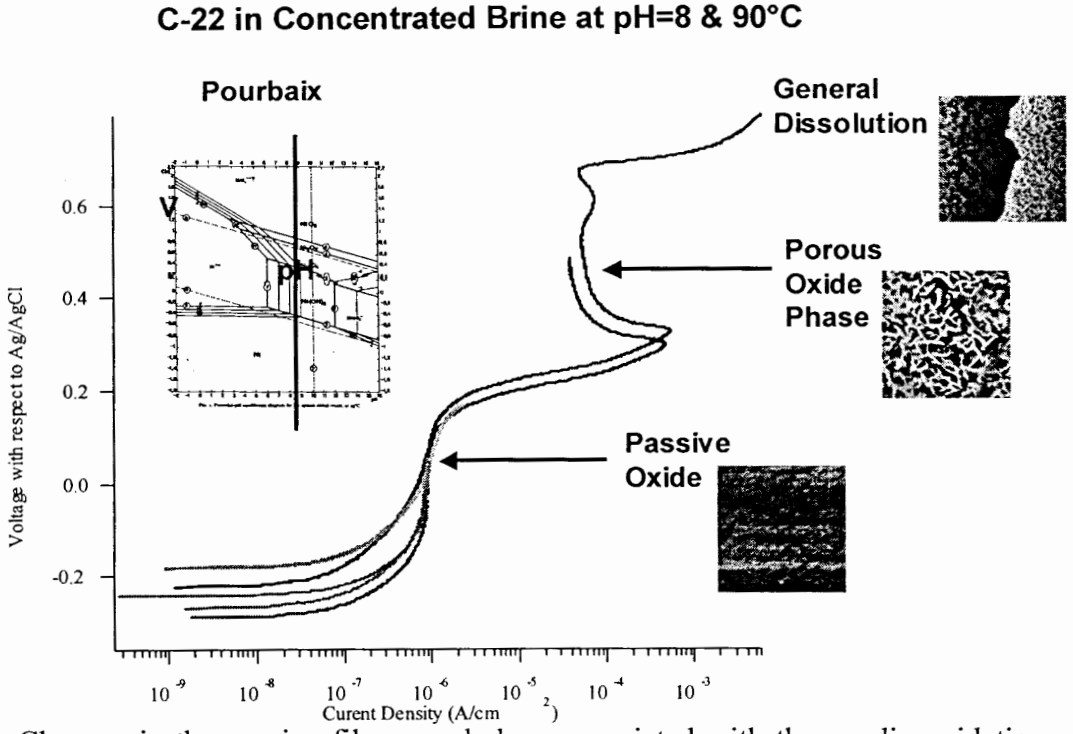

Figure 16. Changes in the passive film morphology associated with the anodic oxidation peak can be observed with the AFM, with a tenacious protective film observed below the anodic peak, and a porous film formed above.

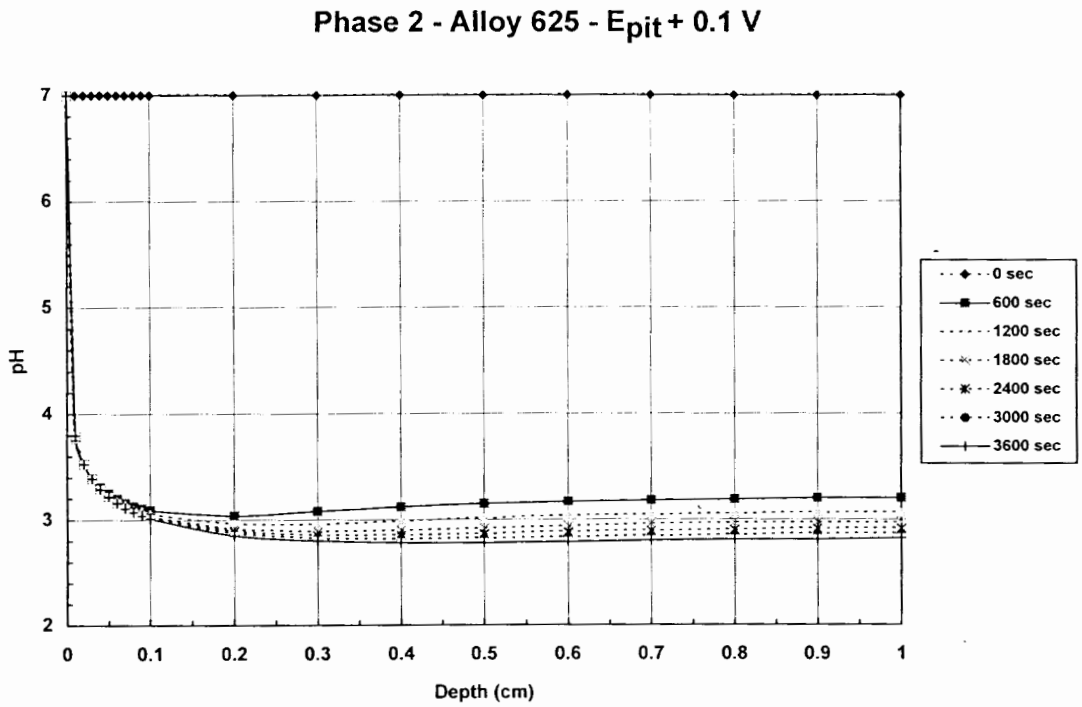

Figure 17. The occluded geometry of a crevice can cause acidification of the solution contained therein, due to field-driven electromigration of hydrogen and chloride ions, and to the hydrolysis reactions of dissolved metal cations inside the crevice. These effects have been simulated with finite element models (E_{pit} is the potential where the passive film is assumed to breakdown).

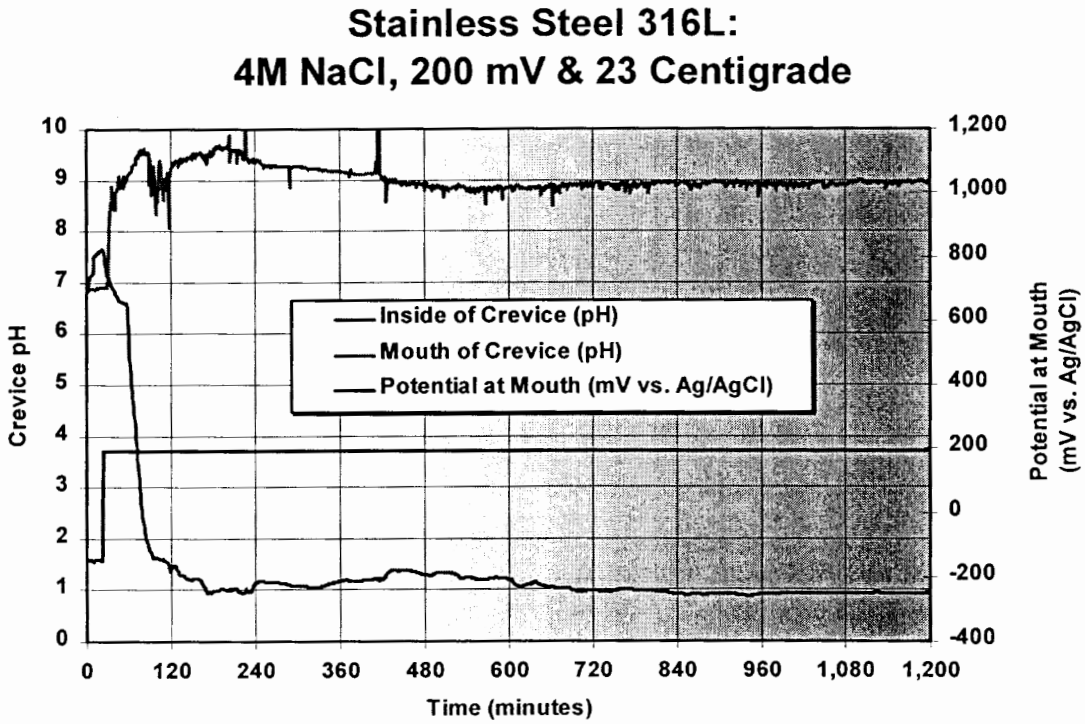

Figure 18. Transient pH profiles have been measured for a variety of alloys and environments, with intentionally creviced samples, and have been used as a basis of validating models.

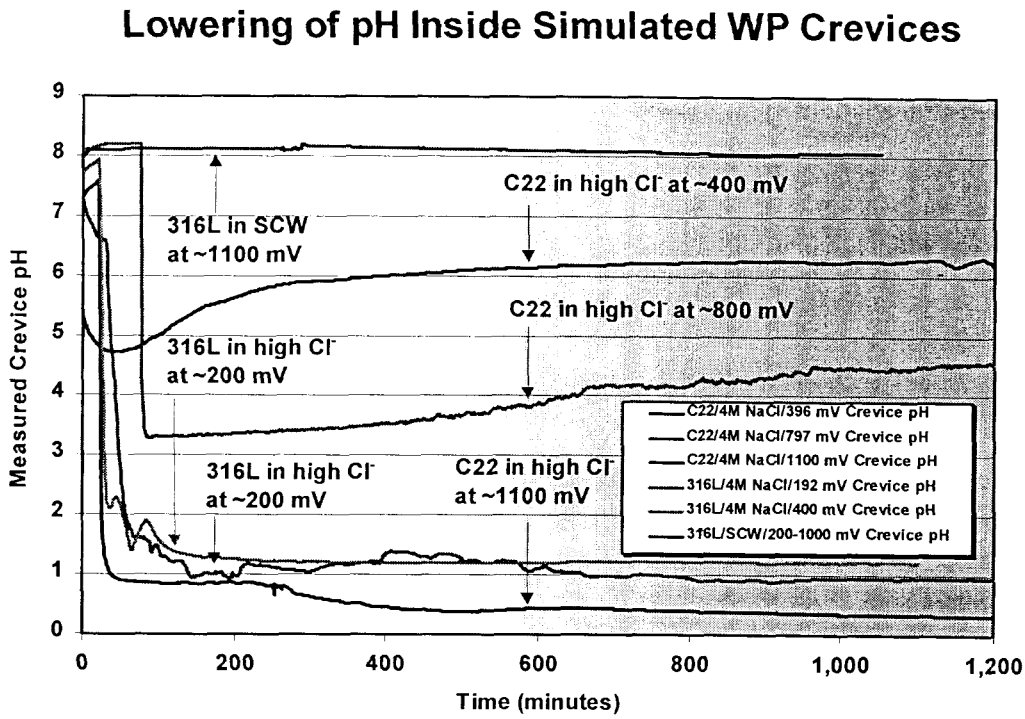

Figure 19. Crevice pH data shows that in situations with buffer and inhibitor ions present (such as SCW), no lowering of the pH occurs.

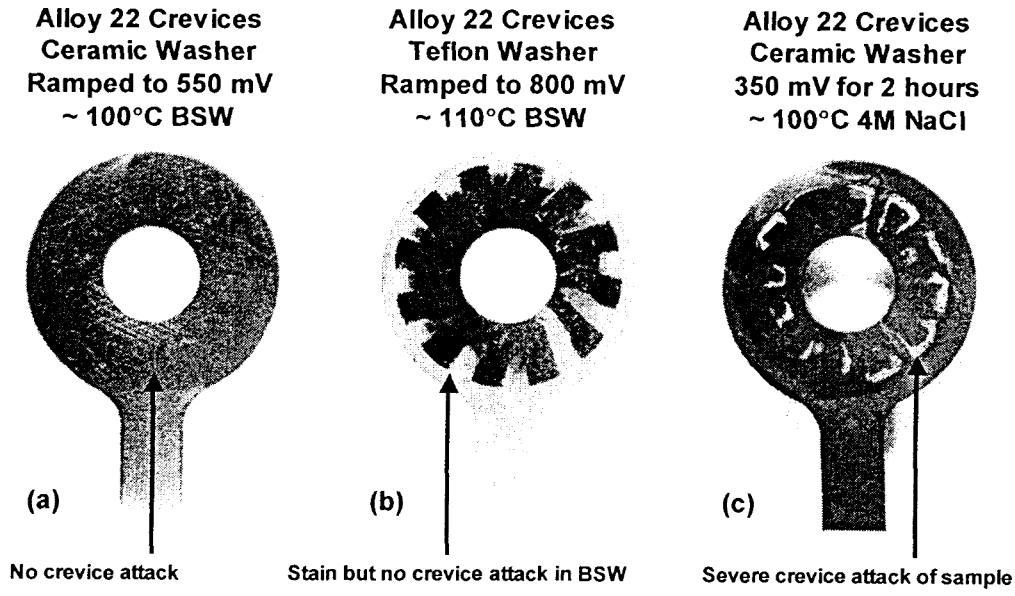

In the case of (a) and (c) above, the potential was increased until a current density of 5 mA cm^{-2} was achieved.

Figure 20. The impact of inhibitor and buffer ions on the crevice corrosion of materials with extreme resistance to localized attack can be elucidated with multiple crevice formers. Buffer and inhibitor ions (as is the case with BSW) prevent crevice corrosion. Solutions of chloride salt near saturation, at similar potential and temperature, undergo crevice attack.

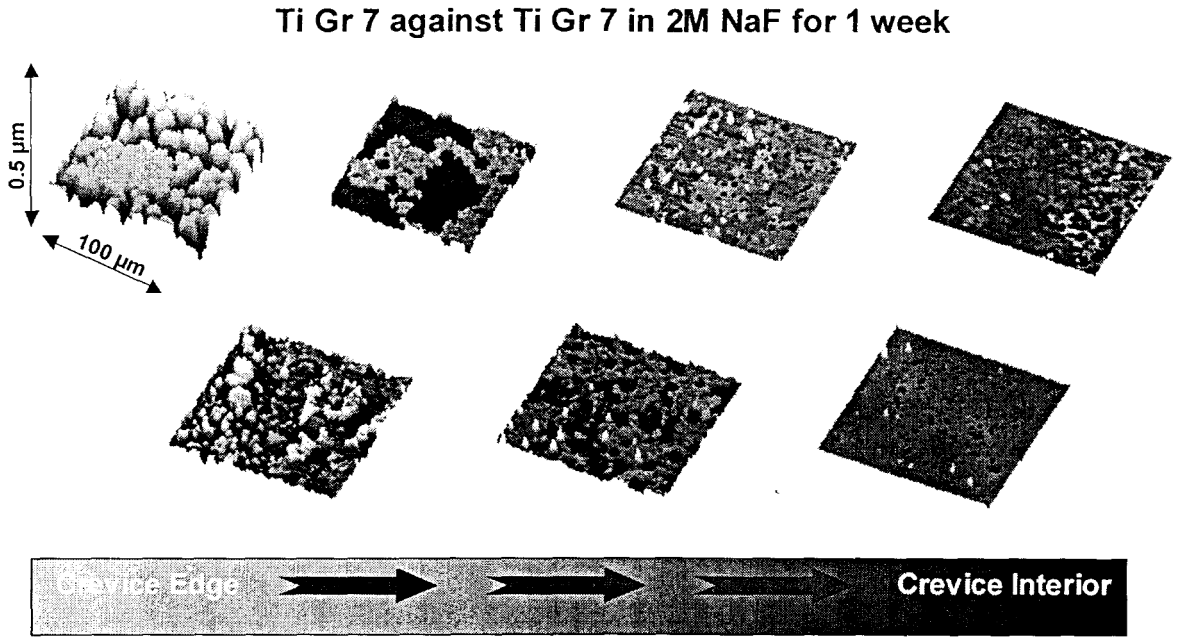

Figure 21. The AFM has been used to observe the crevice attack of titanium alloys exposed to environments with concentrated fluoride salts. This approach provides an extremely sensitive means of assessing susceptibility to crevice attack.

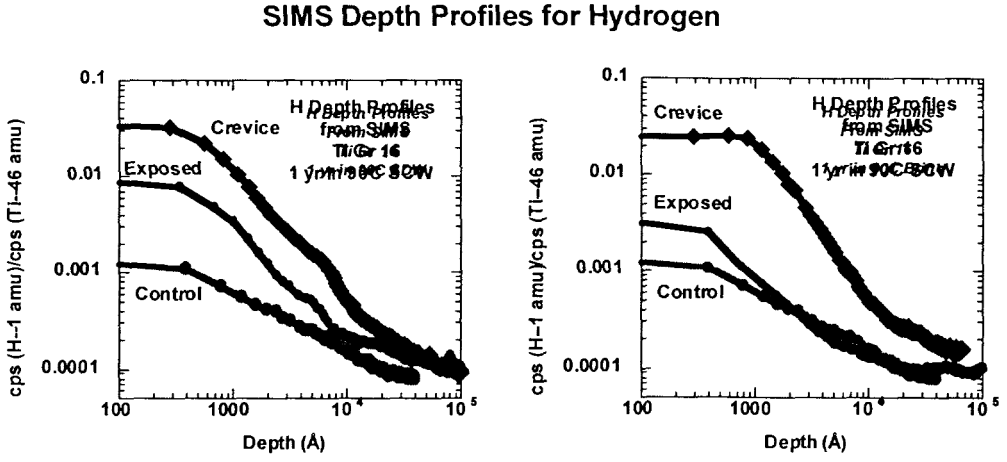

Figure 22. Secondary ion mass spectrometry (SIMS) has been used to measure the hydrogen absorbed by titanium in realistic crevice geometries. Once the hydrogen is absorbed, it can drive hydrogen induced cracking, diffusing down stress gradients.

Microbial Influenced Corrosion (MIC)

Microbial growth can generate various ions that are known to exacerbate corrosion. Some bacteria produce acid (H^+), which tends to dissolve the passive film. Other species oxidize ferrous (Fe^{2+}) to ferric (Fe^{3+}) ion, thereby raising the mixed potential of the surface to levels approaching the threshold for localized attack. Sulfate-reducing bacteria convert sulfate (SO_4^{2-}) to sulfide (S^{2-}), a species known to cause SCC in high-performance nickel based alloys. Ultimately, the impact of MIC will be accounted for by adjusting the corrosion and threshold potentials, pH of the electrolyte, and the sulfide concentration. The extent of MIC is limited by the availability of nutrients and water. We have shown that MIC can enhance corrosion rates of stainless steel Type 304 by a factor of approximately ten (×10).

LLNL has world-class capability in the field of microbial influenced corrosion that can be readily applied to possible problems in power generation systems. As previously done for other systems, microbes can be extracted from power generation systems, cultivated and characterized. Their tendencies to produce acid, sulfide and ferric ion can be determined quantitatively. The acceleration of corrosion processes by microbial growth is included in performance assessment models.

Stress Corrosion Cracking & Hydrogen Induced Cracking

As shown in Figure 24, stress corrosion cracking (SCC) and hydrogen induced cracking (HIC) of materials may occur when a combination of material susceptibility, tensile stress and appropriate environment are present. In the case of HIC of titanium-based alloys, the time-dependent absorption of hydrogen by the material, and the diffusion of hydrogen up stress gradients must be accounted for. This requires the integration of cathodic hydrogen charging models with stress distribution models.

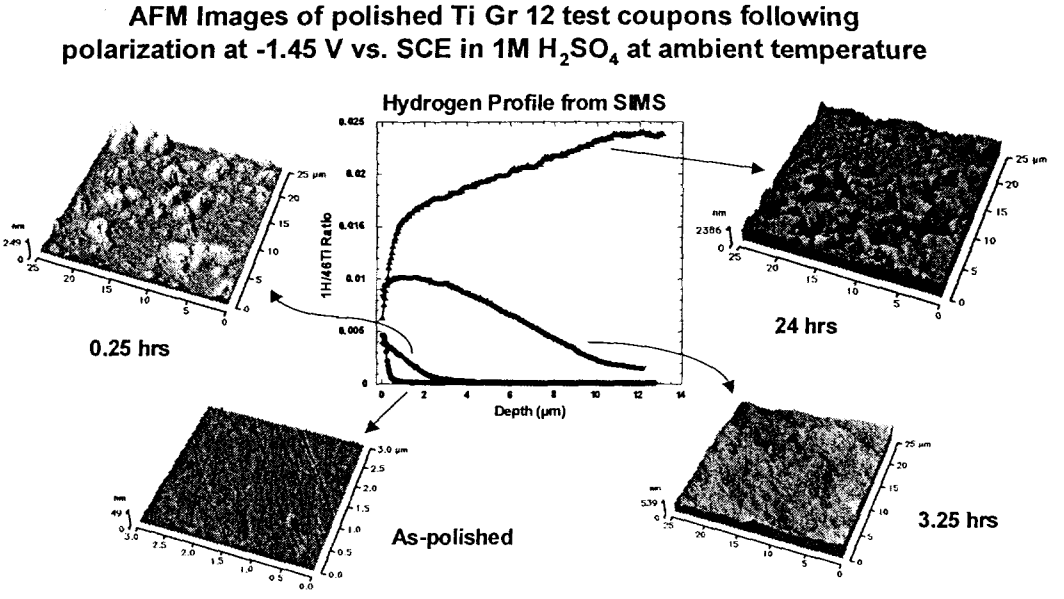

Figure 23. After lowering the electrochemical potential, the formation of sub-surface hydrogen micro-bubbles due to cathodic charging are visible with the AFM.

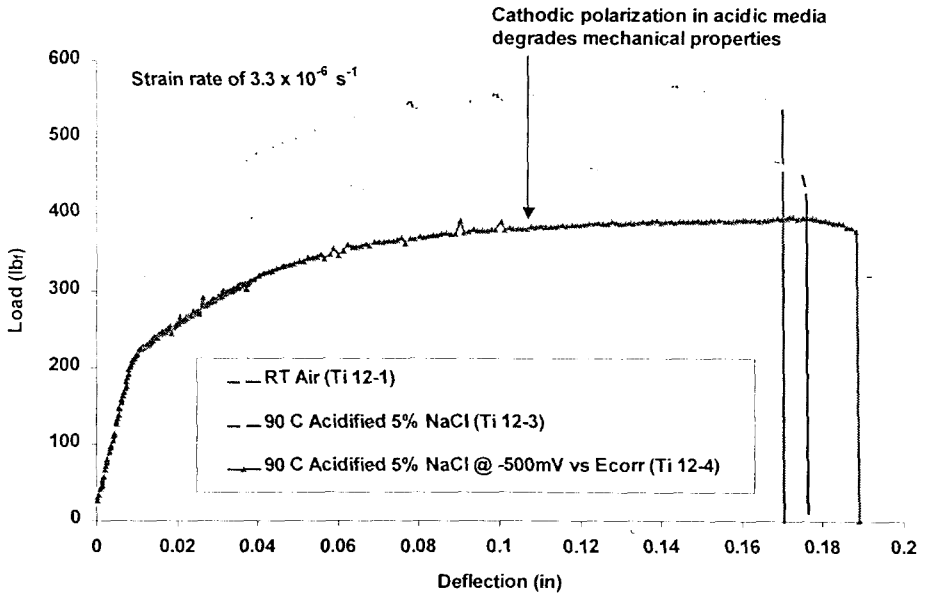

Figure 24. Slow strain rate testing (SSRT) has been used to determine the susceptibility of titanium and other alloys to both SCC and HIC. Straining in acidic chloride solutions and cathodic polarization lowers the maximum load that can be sustained before cracking, which is indicative of susceptibility to hydrogen cracking.

Models have been developed to account for this potentially catastrophic failure mode. The integrated predictive modeling strategy for developed by LLNL for SCC uses one model to predict initiation, and a second to predict crack propagation: the model for crack initiation is based on stress intensity threshold factor criterion ($K_I > K_{ISCC}$); and the model for crack propagation is based on the film-rupture slip-dissolution mechanism. While this approach has been demonstrated for polycrystalline alloys, the applicability to glassy alloys has not yet been established, and would be done as part of the proposed work.

The rate of SCC propagation is dependent upon the local environment and the stress intensity factor at the crack tip. The stresses for initiation and propagation of SCC may be due hydrostatic pressure or other forces. Appropriate stress analysis models and measurements are used to calculate the through-wall stress distribution for the waste package for representative cross sections, including un-welded base metal, and un-annealed welds. This stress distribution is used to calculate a corresponding stress intensity factor distribution for flaws that range in size from zero to the entire thickness of the wall. This stress intensity factor distribution is used as input for the crack initiation model. The SCC initiation model assumes that cracks initiates at pre-existing flaws that develop during fabrication of the waste package, or at flaws that develop during localized corrosion. Experimentally determined values of K_{ISCC} are employed in the initiation model. The rate of SCC propagation is calculated as a function of local environment and stress intensity factor. The time-to-failure is determined by integrating the calculated propagation rate.

To facilitate probabilistic predictions, abstracted models have been developed for SCC and include: 1) a threshold stress for initiation; 2) a crack growth rate as a function of stress and

local exposure conditions, including temperature; 3) crack density; and 4) crack morphology. Crack morphology includes a description of the size of openings. The abstracted models are in a form that is suitable for input to a probabilistic performance assessment model, and includes the uncertainty and variability of the above processes.

Stress Mitigation Techniques

A variety of state-of-the art stress mitigation technologies are also available at LLNL, including laser peening. It has been demonstrated that these new process technologies can be used for the elimination of tensile surface stresses that can lead to SCC and corrosion fatigue. This technology has already been applied to turbine blades for aircraft, with obvious extensions to steam generation equipment. Toshiba has now applied a similar technology to the stress relief of BWR pressure vessels (under water). Work in the theoretical and experimental determination of time-temperature-transformation (TTT) and phase diagrams, and stress distributions in the welds and heat-affected zones, is also exploited to design other stress mitigation approaches, such as localized induction annealing.

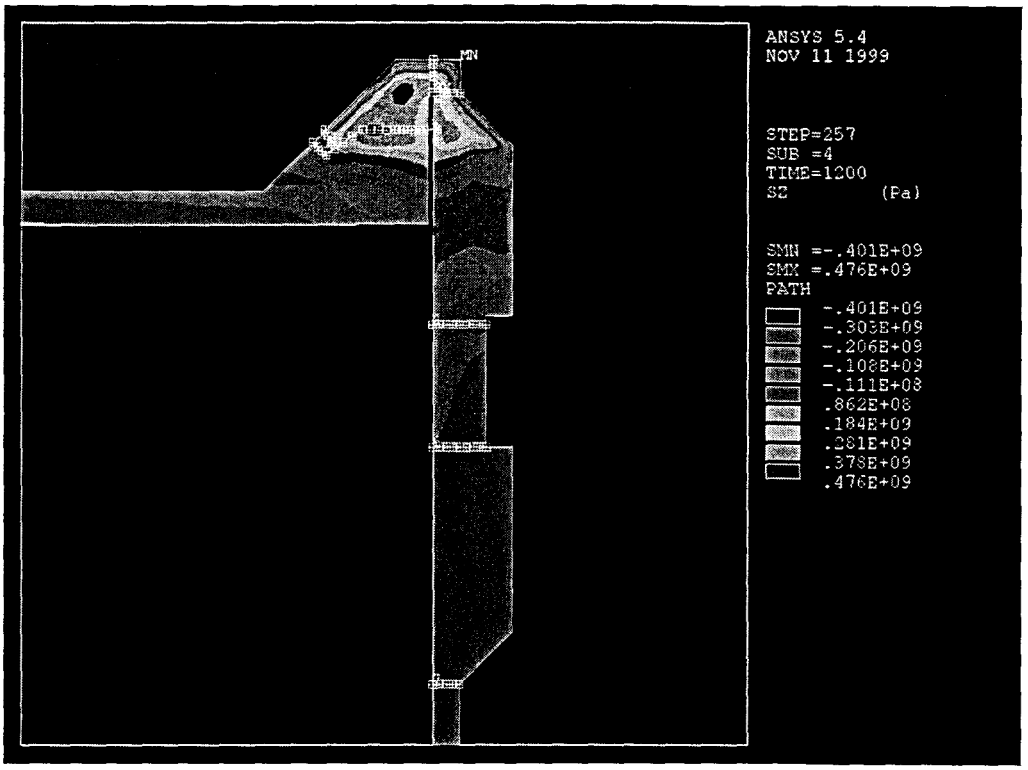

Simulation capability is used to establish conditions for localized induction annealing necessary to prevent SCC in outer closure weld

Figure 25. Once the bounds of thermal annealing are established with an appropriate TTT diagram, the evolution of the stress field at and around welds can be predicted with finite element models. If the surface can be placed under compression through application of localized induction annealing, both SCC and HIC are made impossible.

Laser peening rapidly produces surface layer (2 mm thick) in weld with stress less than 20% of the yield stress - requires less than 4 hours

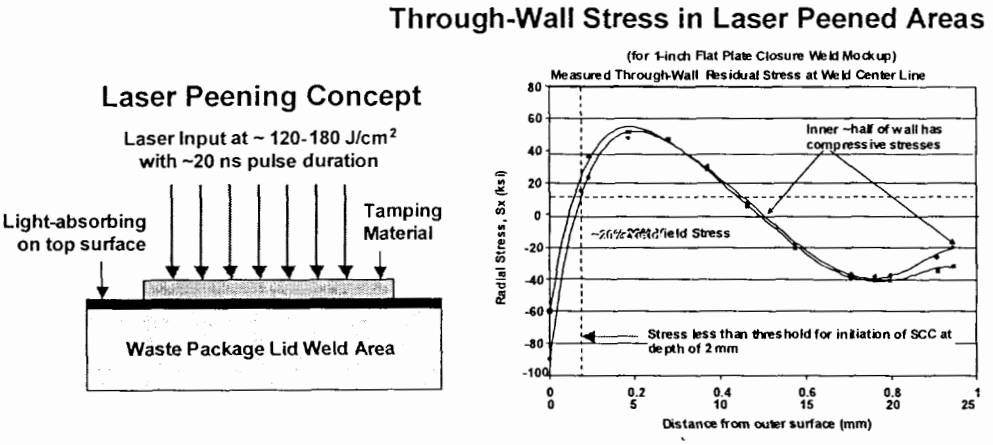

Process optimization may extend depth of stress relief to approximately 3 mm - stress in peened region modeled as polynomial

$$\sigma = A_0 + A_1 x + A_1 x^2 + A_1 x^3$$

Figure 26. Similarly, laser peening can also be used to introduce compressive stress in the surface of welds, thereby making SCC and HIC impossible.

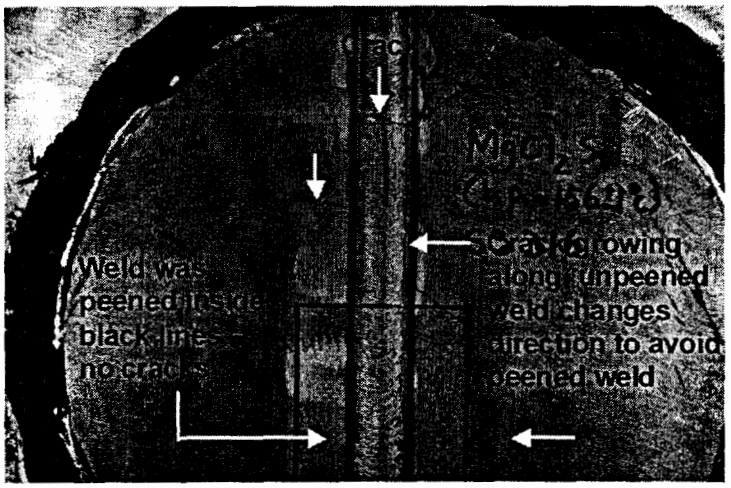

Laser peening has been demonstrated as an effective means of mitigating tensile residual stresses at welds

Exposure of weld in Type 316 stainless steel to boiling $MgCl_2$ for 1 week

Figure 27. Laser peening has been demonstrated to prevent SCC in the classical experiment where a welded Type 316 stainless steel plate is exposed to boiling magnesium chloride for one week.

Coatings for Prevention of Corrosion

A variety of ceramic coatings have been developed to prevent the corrosion of carbon steel substrates. These protective coatings can be applied by conventional plasma spraying, or by a high-velocity oxy-fuel (HVOF) process. As shown in Figures 28 and 29, ceramic coatings produced with the high-velocity oxy-fuel (HVOF) process have little interconnected porosity, whereas coatings produced with conventional plasma spray have substantial interconnected porosity, and make poor barriers to corrosion. After exposure of carbon steel samples with HVOF coatings to brine at 90°C for six months, no corrosion was observed at the metal-ceramic interface. This is in sharp contrast to the corrosion observed with conventional plasma sprayed coatings.

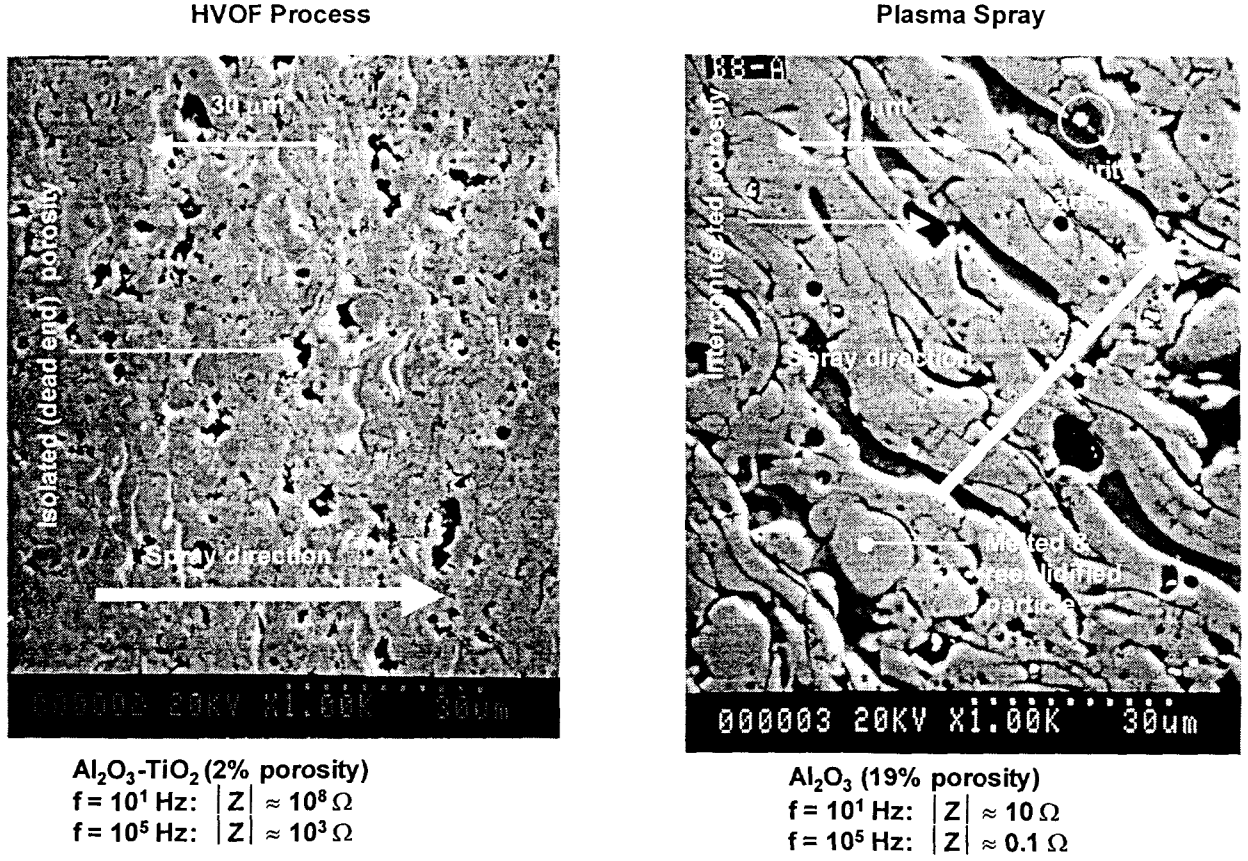

Figure 28. Ceramic coatings produced with the high-velocity oxy-fuel (HVOF) process have little interconnected porosity, whereas coatings produced with conventional plasma spray have substantial interconnected porosity, and make poor barriers to corrosion.

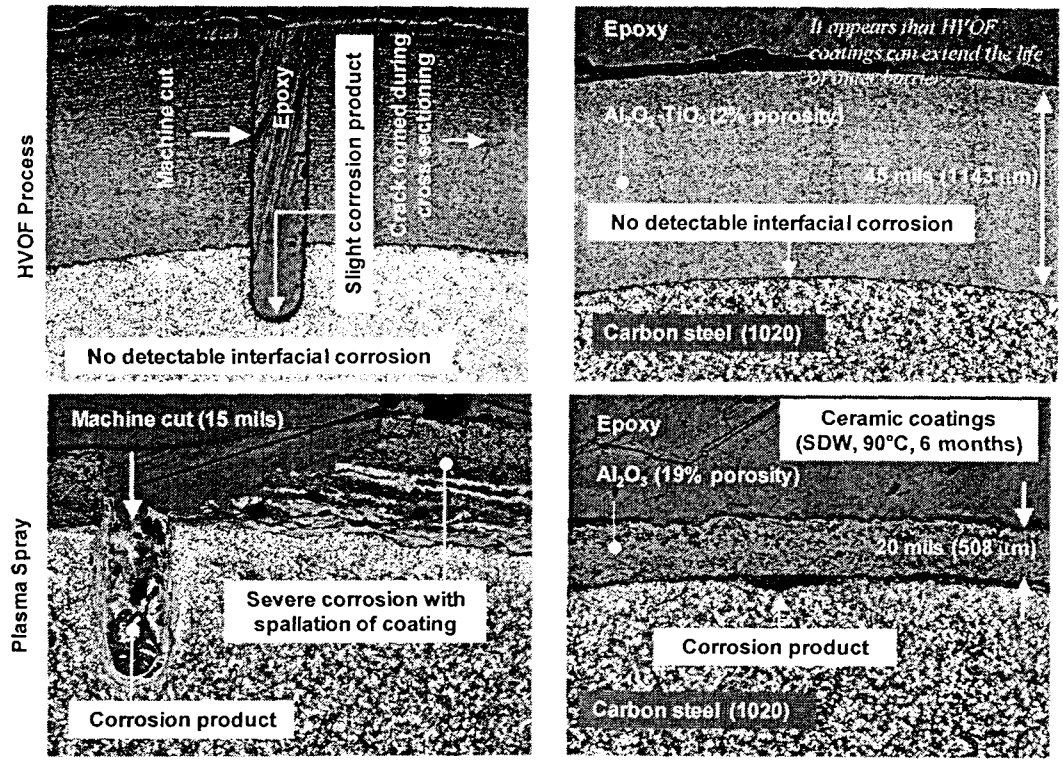

Figure 29. As seen in Figure 28, eramic coatings produced with the high-velocity oxy-fuel (HVOF) process have little interconnected porosity, whereas coatings produced with conventional plasma spray have substantial interconnected porosity, and make poor barriers to corrosion. After exposure of carbon steel samples with HVOF coatings to brine at 90°C for six months, no corrosion was observed at the metal-ceramic interface. This is in sharp contrast to the corrosion observed with conventional plasma sprayed coatings.

Summary

DARPA has now developed a number of advanced materials for military applications, including amorphous metals and titanium-based alloys. Equipment made from these materials can undergo degradation due to thermal aging, uniform corrosion, pitting, crevice corrosion, denting, stress corrosion cracking, corrosion fatigue, hydrogen induced cracking and microbial influenced corrosion. Amorphous alloys have exceptional resistance to corrosion, due in part to the absence of grain boundaries, but can undergo crystallization and other phase instabilities during heating and welding. Titanium alloys are extremely corrosion resistant due to the formation of a tenacious passive film of titanium oxide, but is prone to hydrogen absorption in crevices, and hydrogen induced cracking after hydrogen absorption. Accurate predictions of equipment reliability, necessary for strategic planning, requires integrated models that account for all relevant modes of attack, and that can make probabilistic predictions. Once developed, model parameters must be determined experimentally, and the validity of models must be established through careful laboratory and field tests. Such validation testing requires state-of-the-art surface analytical techniques, as well as electrochemical and fracture mechanics tests.

In addition to the classic techniques for screening materials and environments, new approaches are also being explored. These include methodologies used in combinatorial synthesis, based on large-scale microelectrode arrays, with each element supplied by a micro-fluidic electrolyte mixing system. Multiplexed multi-channel potentiostats are used to determine the polarization curves for each element. Large combinations of alloy and/or electrode composition can be explored, with the total number of combinations on the order of 10,000 (10^4). Precise water chemistries causing materials failure can be easily found through this approach, while new alloy compositions immune to such failure can be quickly identified. Partnerships exist in the San Francisco Bay Area to further enable this novel, cutting-edge approach to corrosion research.